

**Supporting information**

**Revealing the role of nitrogen dopant in tuning electronic  
and optical properties of graphene quantum dot from  
TD-DFT study**

Min Yang,<sup>†,‡</sup> Zan Lian,<sup>†,‡</sup> Chaowei Si,<sup>†,‡</sup> and Bo Li<sup>\*,†</sup>

<sup>†</sup>Shenyang National Laboratory for Materials Science, Institute of Metal Research, Chinese Academy of Sciences, Shenyang 110016, Liaoning, People's Republic of China

<sup>‡</sup>School of Materials Science and Engineering, University of Science and Technology of China, Shenyang 110016, Liaoning, People's Republic of China

**Table S1** Calculated HOMO-LUMO gap and absorption color corresponding to wavelength.

GQDs	HOMO-LUMO gap (eV)	color
C6	6.80	ultraviolet
C24	4.04	ultraviolet
C32	2.93	ultraviolet
C54	2.82	Violet
C66	2.06	blue
C78	1.49	green
C54-g-1	1.16	blue
C54-g-2	1.14	blue
C54-g-3	0.90	red
C54-g-4	1.09	blue
C54-g-5	1.42	Infrared
C54-g-6	3.63	red
C54-pyd-1	1.39	Violet
C54-pyd-2	1.64	Violet
C54-pyd-3	0.91	red
C54-pyd-4	0.71	green
C54-pyd-5	1.31	red
C54-pyd-6	2.15	green
C42	1.90	red
C42-pyo-1	1.16	Infrared
C42-pyo-2	1.14	blue
C42-pyo-3	0.90	orange
C42-pyo-4	1.09	ultraviolet
C42-pyo-5	1.42	ultraviolet
C42-pyo-6	3.63	ultraviolet

**Table S2** Excitation energies, wavelengths, oscillator strengths, transition coefficients, and associated eigenvalues of the dominated excitation in GQDs.

GQDs	Dominant excitation	Excitation energy/eV	Wave length(nm)	Oscillator strength ( $f$ )	Transition coefficients	$\lambda_i$
C54	S3	2.90	427.00	0.93	H-1→L+1 0.48 H→L 0.48	0.46 0.46
	S4	2.90	427.00	0.93	H-1→L 0.48	0.46 0.46
	S12	2.71	456.97	0.46	H-1→L+1 0.63 H →L+7 -0.19 H-2→L+1 0.64	0.81 0.83
C54-g-2	S14	2.86	433.67	0.37	H-1→L+3 -0.17	
C54-g-3	S19	1.97	629.24	0.07	$\alpha H-1 \rightarrow \alpha H+5$ -0.18 $\alpha H \rightarrow \alpha L+4$ 0.81 $\beta H \rightarrow \beta L+4$ 0.13 $\beta H \rightarrow \beta L+7$ -0.47	0.48 1.29
C54-g-4	S14	2.54	488.40	0.36	H-2→L 0.52 H→L+6 -0.37	0.54 0.29
C54-g-5	S14	1.43	869.47	0.04	$\alpha H \rightarrow \alpha L+2$ 0.79 $\beta H-2 \rightarrow \beta L$ 0.17 $\beta H \rightarrow \beta L$ -0.13	1.8 0.12
C54-pyd-2	S10	2.93	422.59	0.63	L-1→H 0.66 L→H+1 0.19	0.88
	S17	3.50	354.47	0.38	H-3→L+1 0.63 H-2→L -0.17	0.81
C54-pyd-3	S10	1.64	758.22	0.17	$\alpha H-1 \rightarrow \alpha L+1$ 0.59 $\beta H \rightarrow \beta L+1$ -0.33 $\beta H \rightarrow \beta L+2$ -0.37	0.73 0.53
C54-pyd-4	S11	2.34	529.95	0.58	H-1→L+1 0.29 H→L+5 0.56	0.67 0.30
C54-pyd-5	S13	1.87	662.50	0.15	$\alpha H-2 \rightarrow \alpha L+1$ 0.65 $\beta H-1 \rightarrow \beta L+2$ 0.60 $\beta H \rightarrow \beta L+1$ 0.21	0.91 0.78

**Table S3** Excitation energies, wavelengths, oscillator strengths, transition coefficients, and associated eigenvalues of the dominated excitation in GQDs.

GQDs	Dominant excitation	Excitation energy/eV	Wave length(nm)	Oscillator strength ( <i>f</i> )	Transition coefficients	$\lambda_i$
C42	S15	1.73	715.49	0.16	H→L+1 0.28 H→L+2 0.47	0.72
	S12	2.35	526.68	0.22	H-4→L 0.39 H-3→L -0.290	0.67 0.25
	S14	2.62	473.80	0.23	H-6→H+1 0.60 H-3→H+1 -0.15	0.80
C42-pyo-2	S18	2.05	603.74	0.10	$\alpha H-6 \rightarrow \alpha L$ 0.47	0.36
					$\alpha H-2 \rightarrow \alpha L$ -0.32 $\beta H-5 \rightarrow \beta L+1$ -0.43	0.48
C42-pyo-3	S15	3.40	364.47	0.33	H-1→L+2 0.57	0.64
					H→L+3 -0.38	0.30
	S16	3.57	347.65	0.30	H-1→L+2 0.37	0.64
					H→L+3 0.56	0.27
	S19	3.44	360.68	0.19	$\alpha H-2 \rightarrow \alpha L$ 0.29	0.25
					$\alpha H-1 \rightarrow \alpha L+2$ 0.30 $\beta H-10 \rightarrow \beta L$ 0.43	0.21 0.14
C42-pyo-4	S20	3.45	359.16	0.21	$\beta H-1 \rightarrow \beta L+1$ 0.32	0.32
					$\alpha H-2 \rightarrow \alpha L+1$ 0.48	0.31
					$\alpha H \rightarrow \alpha L+2$ 0.47 $\beta H-1 \rightarrow \beta L+2$ -0.32 $\beta H \rightarrow \beta L+1$ 0.24	0.39 0.15

**Table S4** The hybridization of nitrogen-bonded carbon of nitrogen doped GQDs and carbon-bonded carbon of pristine GQDs.

system	bond	number of carbon atoms	Hybrids
C54	C 2-C 6	6	s (34.69%) p 1.88(65.28%)
	C 2-C 8	8	s (34.69%) p 1.88(65.28%)
	C 38-C 39	38	s (33.09%) p 2.02(66.87%)
	C 39-C 46	46	s (33.40%) p 1.99(66.56%)
C42	N 39-C 48	48	s (33.40%) p 1.99(66.56%)
	C 24-C 25	24	s (33.91%) p 1.95(66.05%)
	C 25-C 26	26	s (33.85%) p 1.95(66.10%)
	C 38-N 39	38	s (27.47%) p 2.64(72.42%)
g-1	N 39-C 46	46	s (26.75%) p 2.73(73.14%)
	N 39-C 48	48	s (26.75%) p 2.73(73.14%)
pyd-1	N 2-C 7	7	s (27.58%) p 2.62(72.31%)
	N 2-C 9	9	s (27.58%) p 2.62(72.31%)
pyo-1	C 24-N 25	24	s (27.20%) p 2.67(72.70%)
	N 25-C 26	26	s (26.94%) p 2.71(72.93%)

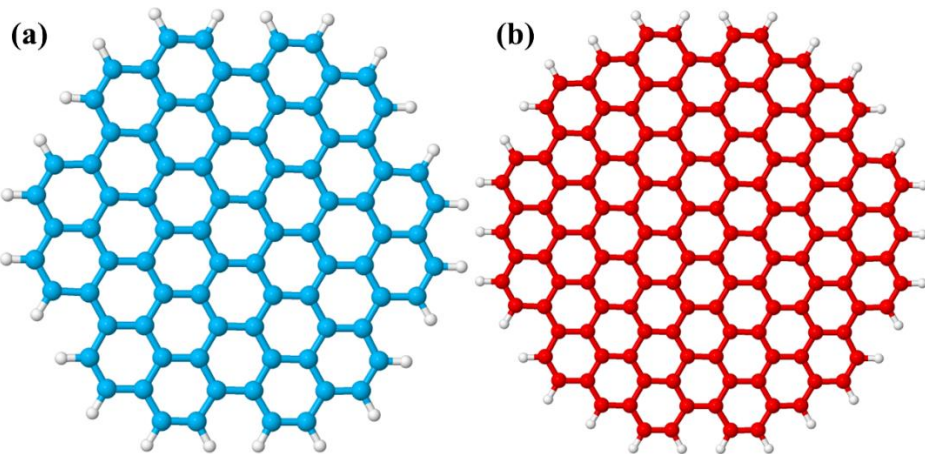


**Fig.S1** The Optimized structure of pristine GQDs with (a) 84 and (b) 138 carbon atoms.

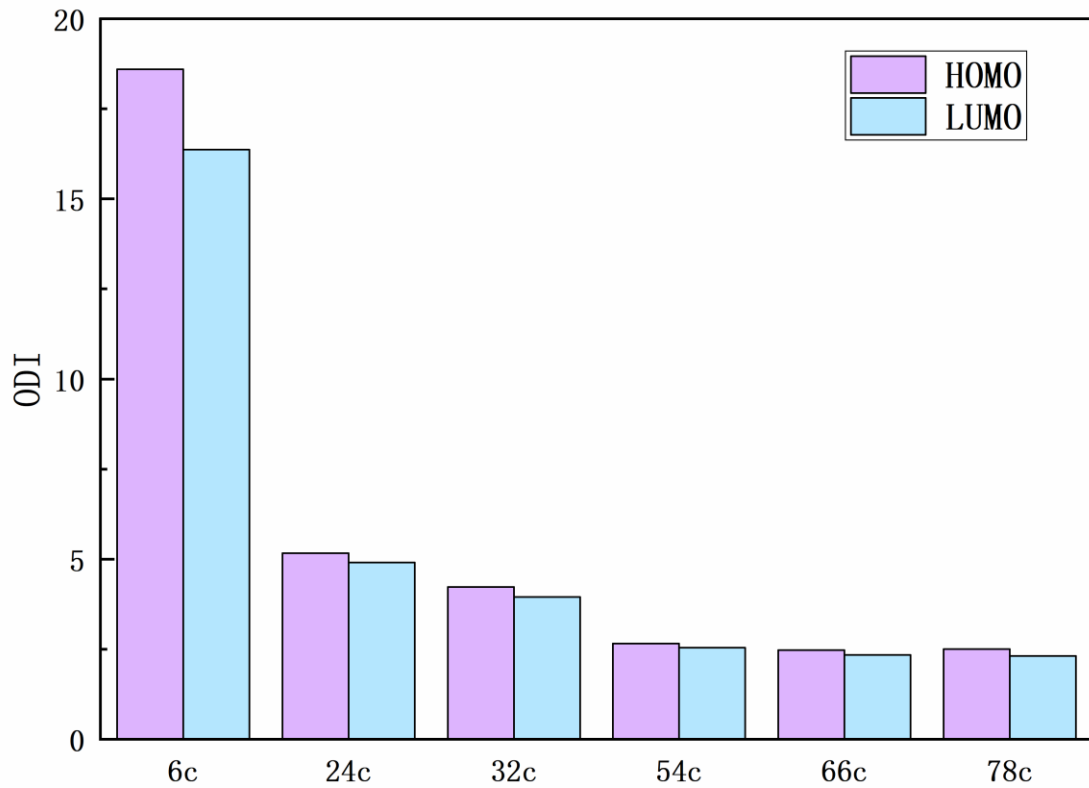


**Fig.S2** Orbital delocalization index (ODI) of pristine GQDs with different size. The smaller the value, the higher the degree of delocalization.

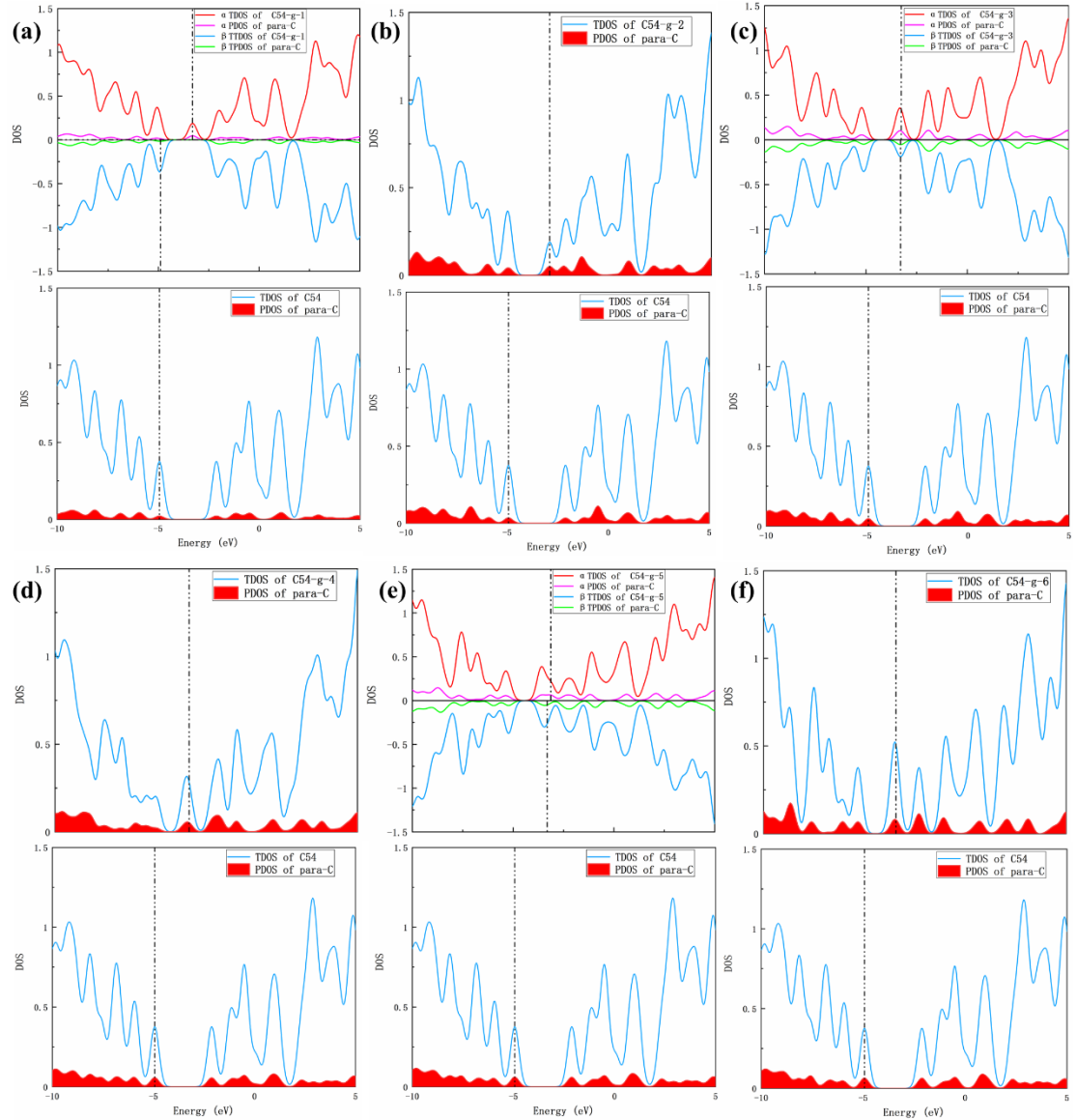


**Fig.S3** Density of state (DOS) of graphitic N-doped GQDs. At the bottom, the DOS of pristine C54-GQDs are shown. (The vertical dashed lines indicate the position of the HOMO level. The DOS is plotted with a Gaussian width of 0.01 eV).

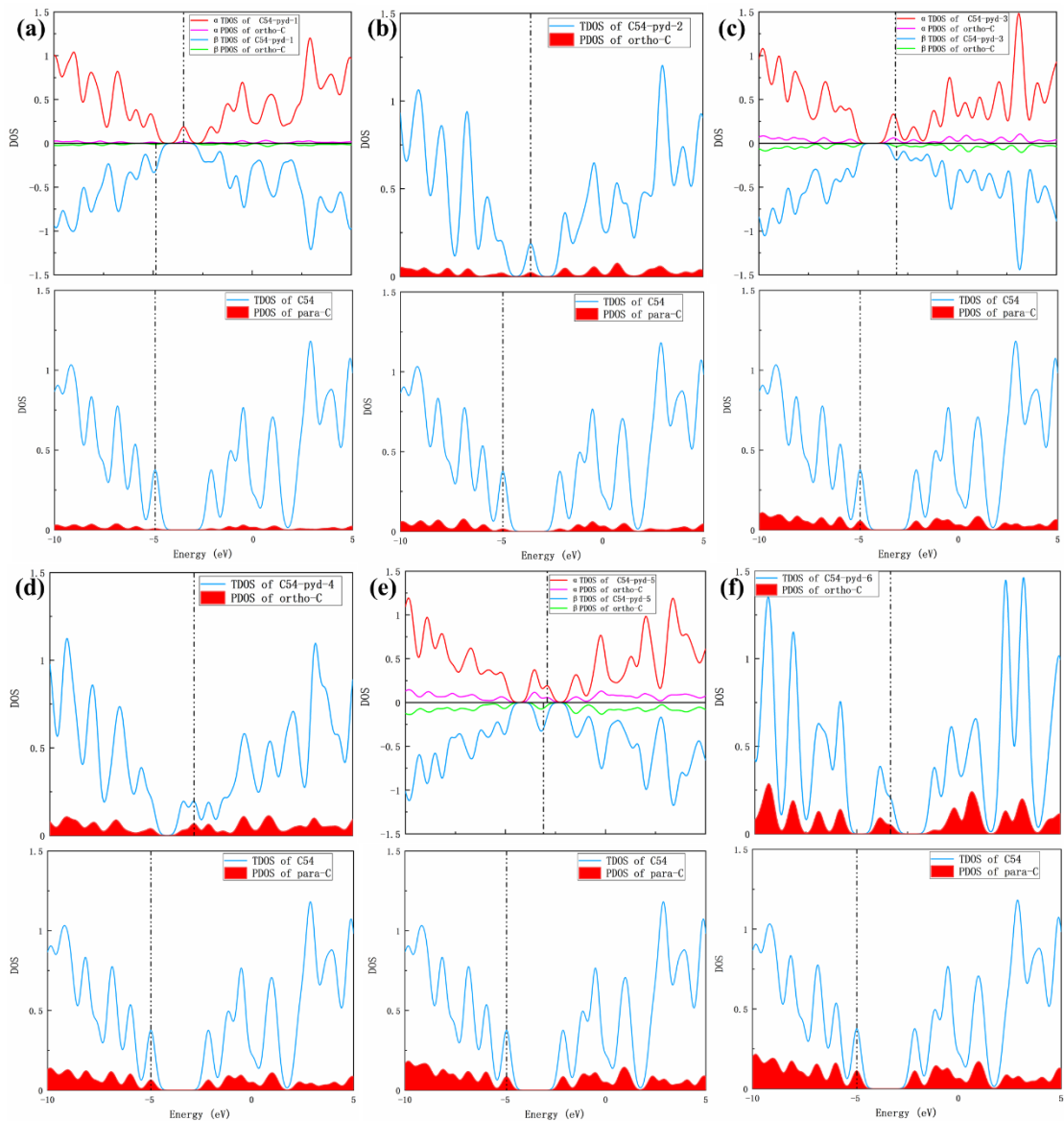


**Fig.S4** Density of state (DOS) of pyridinic N-doped GQDs. At the bottom, the DOS of pristine C54-GQDs are shown. (The vertical dashed lines indicate the position of the HOMO level. The DOS is plotted with a Gaussian width of 0.01 eV).

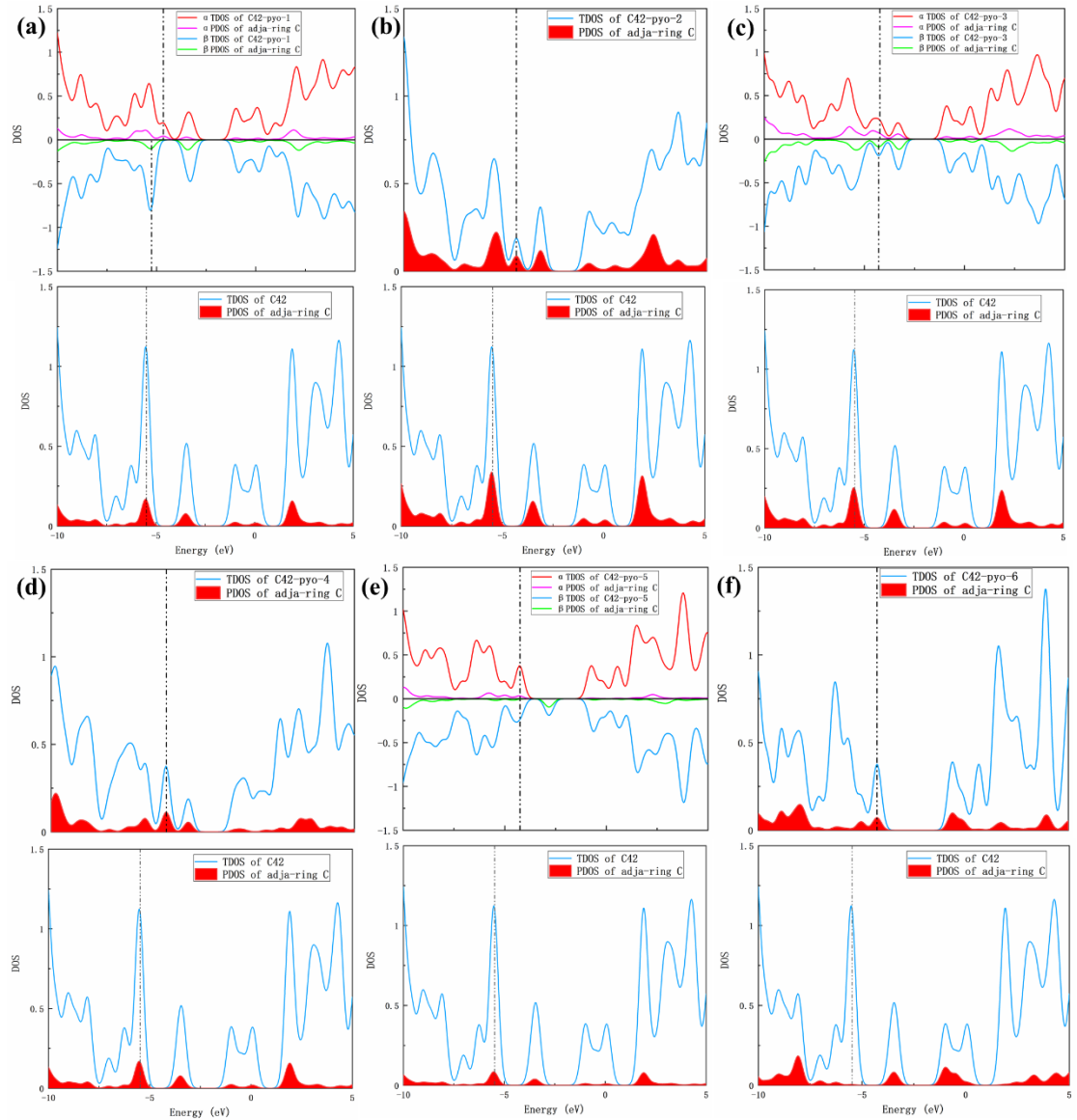


**Fig.S5** Density of state (DOS) of pyrrolic N-doped GQDs. At the bottom, the DOS of pristine C42-GQDs are shown. (The vertical dashed lines indicate the position of the HOMO level. The DOS is plotted with a Gaussian width of 0.01 eV).

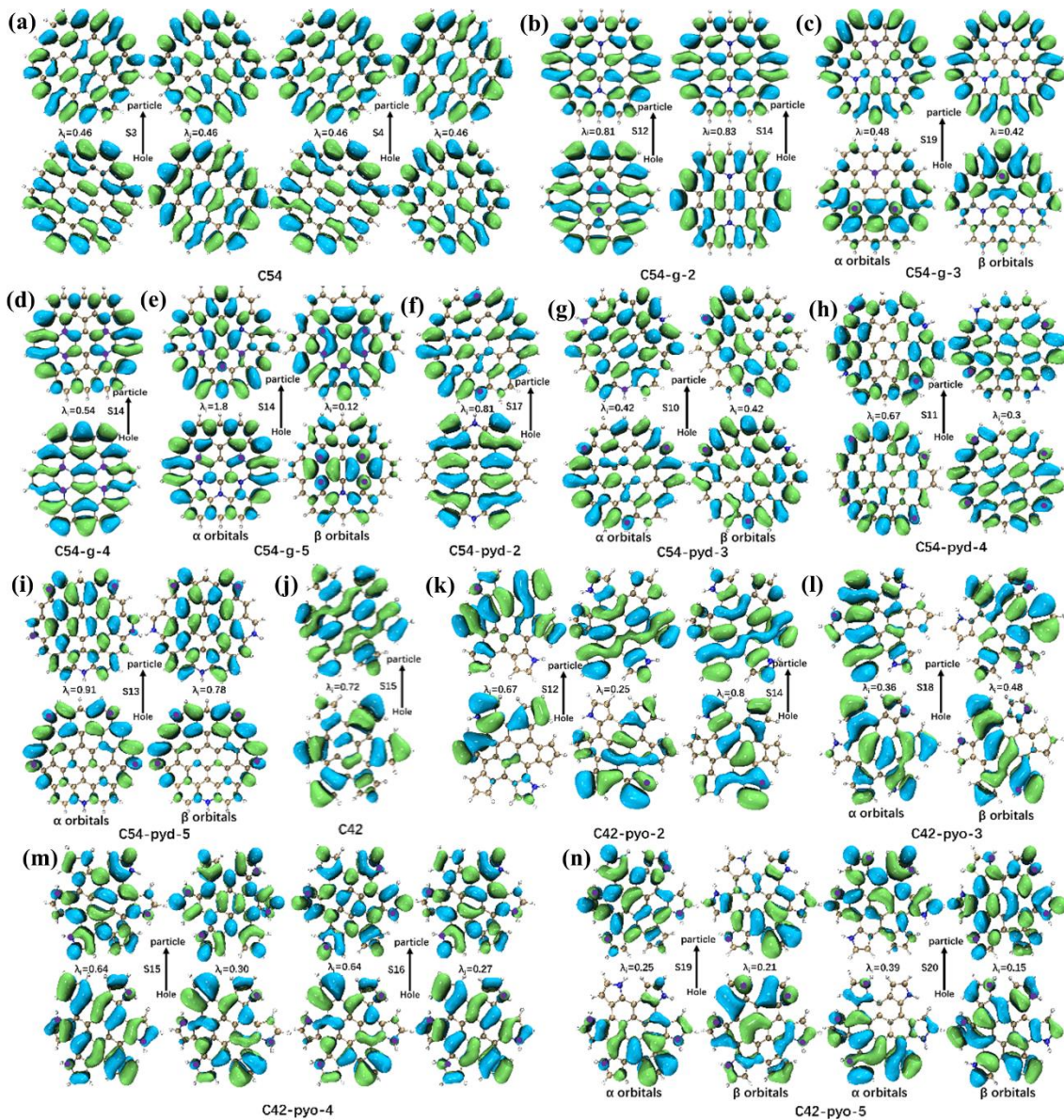


**Fig.S6** The NTO pairs for the prominent excited states of doped GQDs. For this state the “hole” is below, and the “particle” is on top; the values represent the associated eigenvalue ( $\lambda_i$ ).

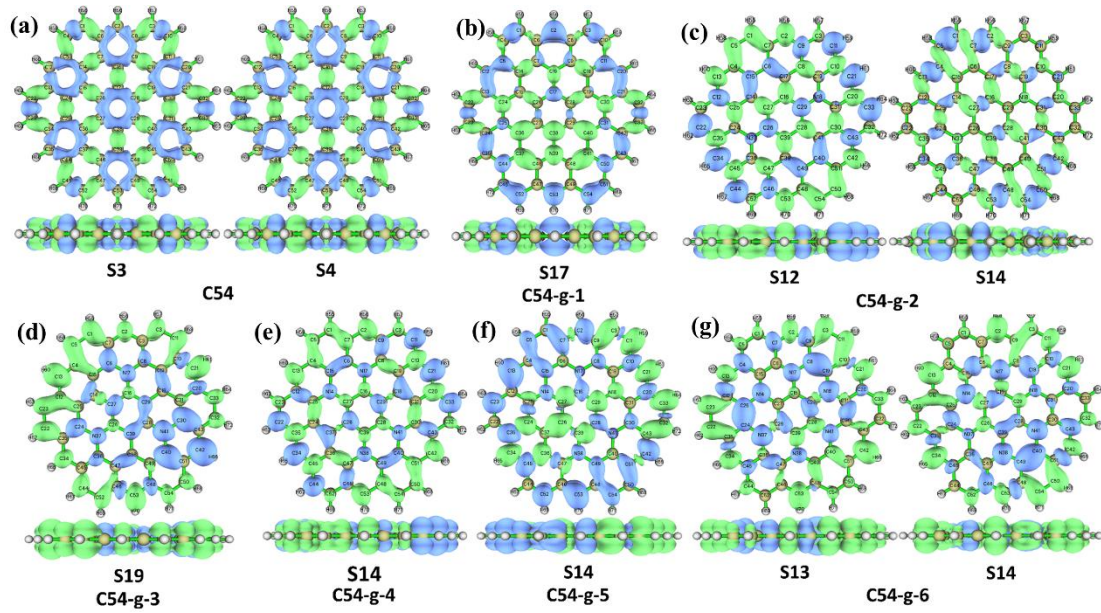


**Fig.S7** Representation of the electron difference density between the dominant excited state and the ground state for C54 and graphitic nitrogen doping GQDs. At the bottom, the lateral views are shown. (The blue area plots the surface where the value of the difference density is -0.0004, the green area plots the surface where the value of the difference density is +0. 0004.)

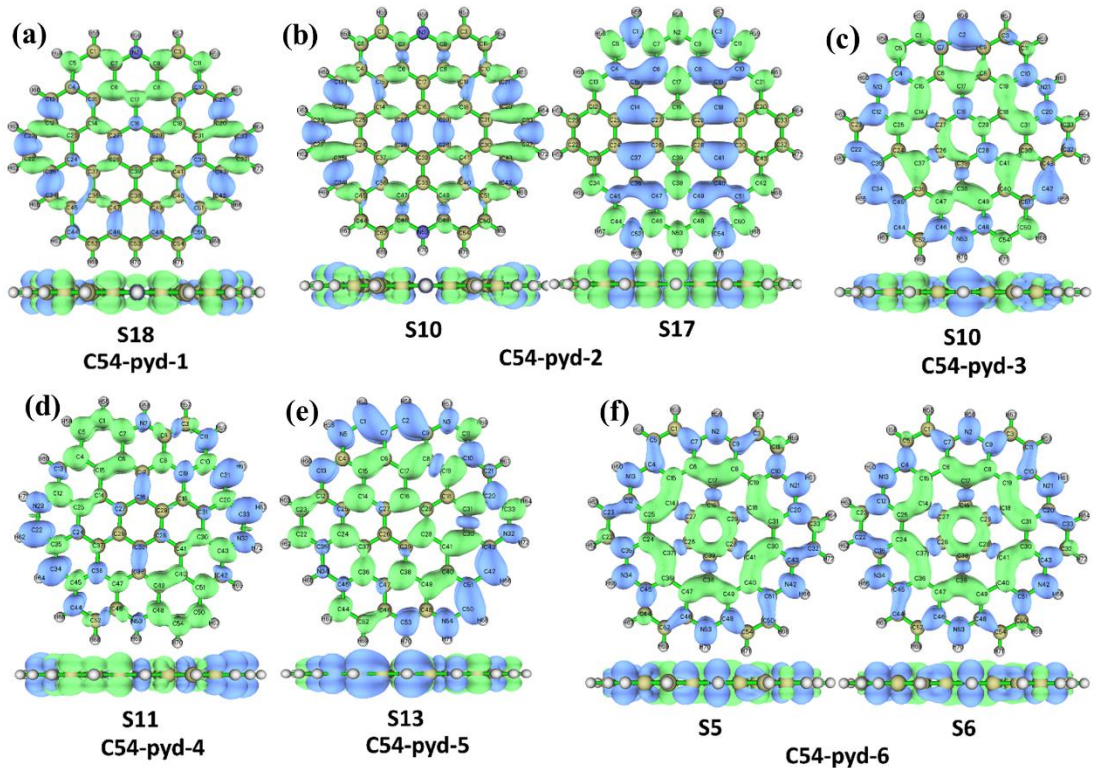


**Fig.S8** Representation of the electron difference density between the dominant excited state and the ground state for pyridinic nitrogen doping GQDs. At the bottom, the lateral views are shown. (The blue area plots the surface where the value of the difference density is -0.0004, the green area plots the surface where the value of the difference density is +0. 0004.)

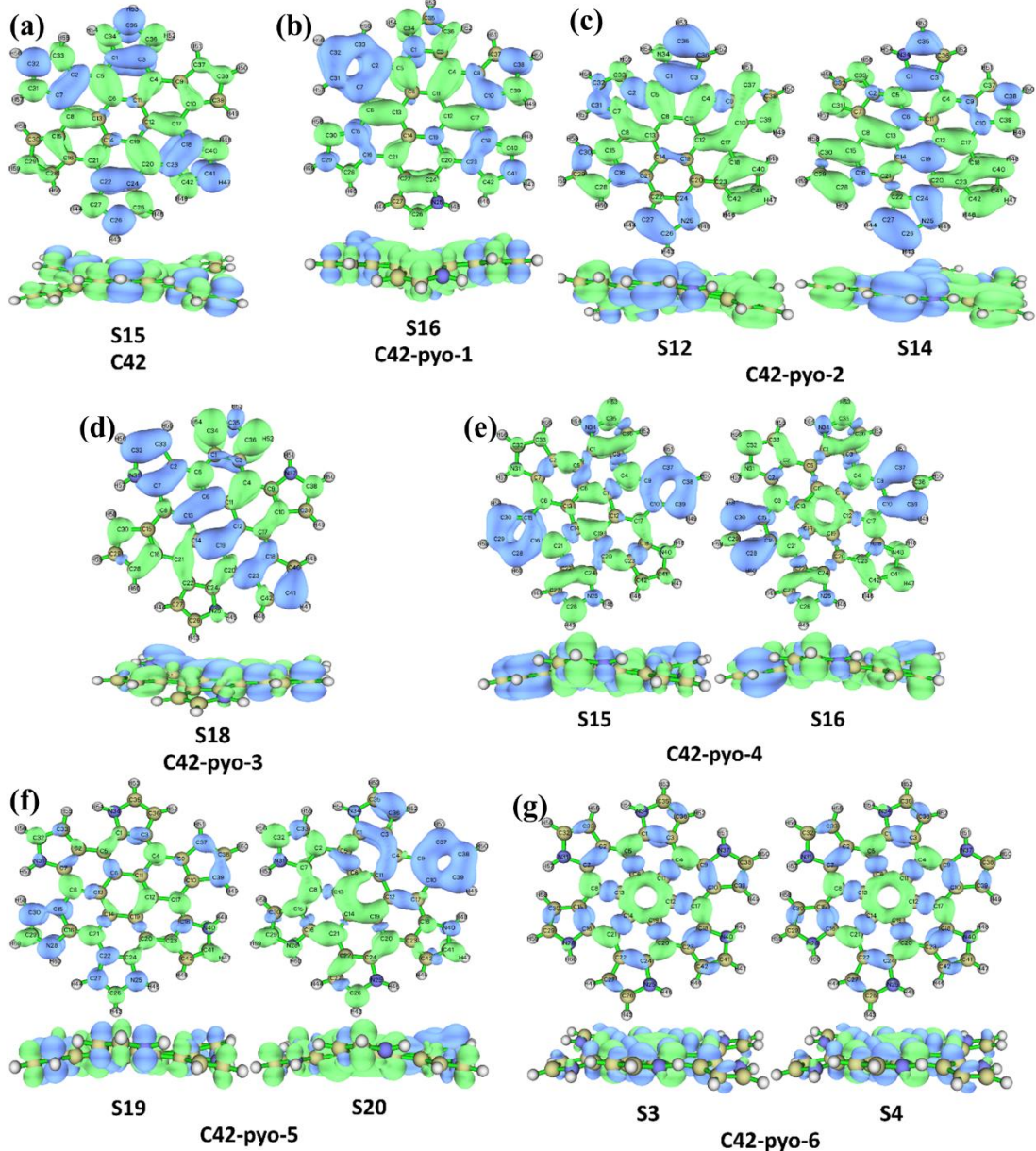


**Fig.S9** Representation of the electron difference density between the dominant excited state and the ground state for C42 and pyrrolic nitrogen doping GQDs. At the bottom, the lateral views are shown. (The blue area plots the surface where the value of the difference density is -0.0004, the green area plots the surface where the value of the difference density is +0.0004.)

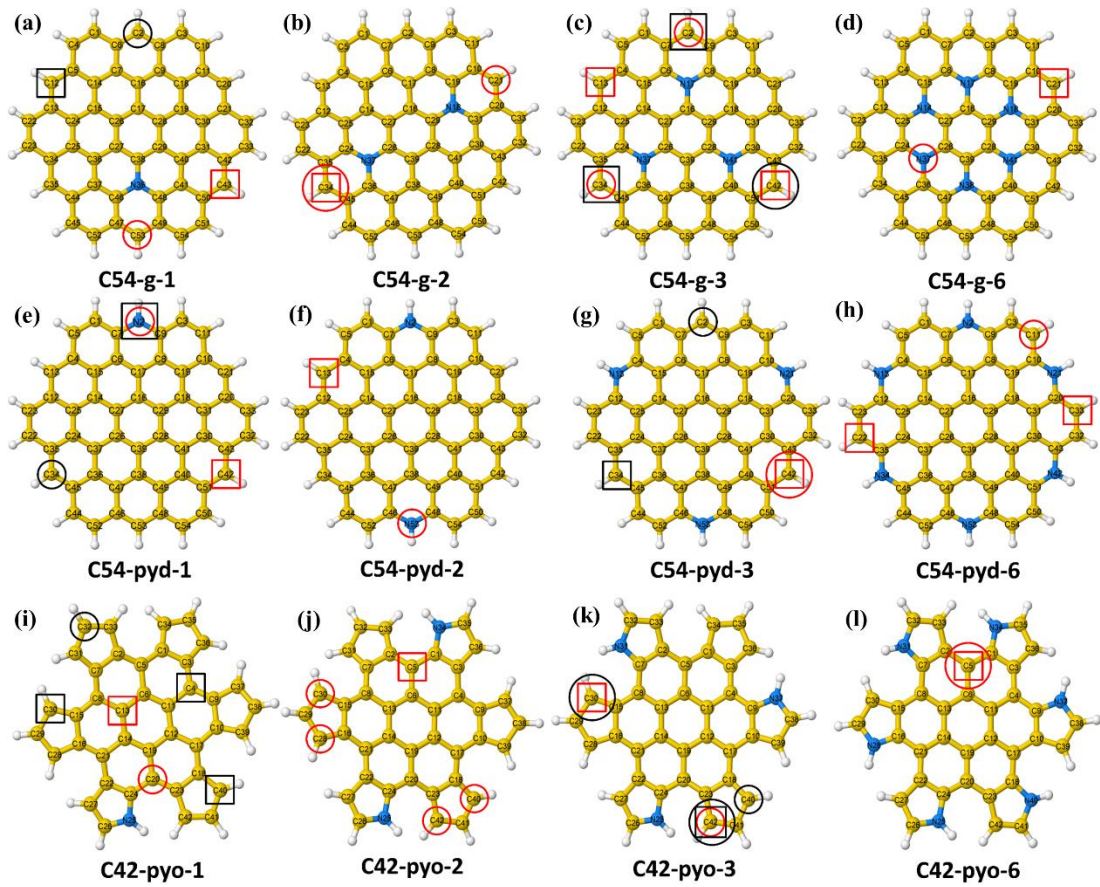


**Fig.S10** Atomic contributions to HOMO and LUMO. The red circle marks the atom that contributes most to alpha HOMO, the red square marks the atom that contributes most to alpha LUMO; the black circle marks the atom that contributes most to beta HOMO, and the black square marks atoms contributes most to beta LUMO. Atoms in blue represent nitrogen, and atoms in white represent hydrogen, and in yellow represent carbon.

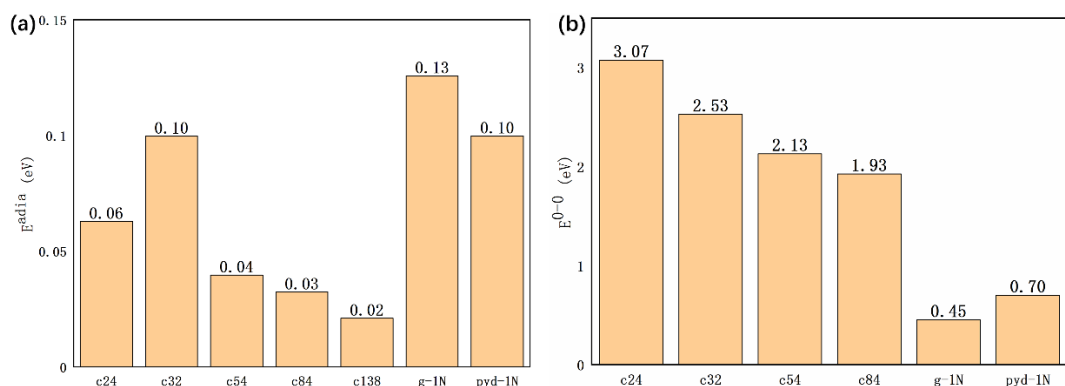


**Fig.S11** The  $E^{0-0}$  and  $E^{adia}$  of different size of pristine GQDs and nitrogen doping GQDs.

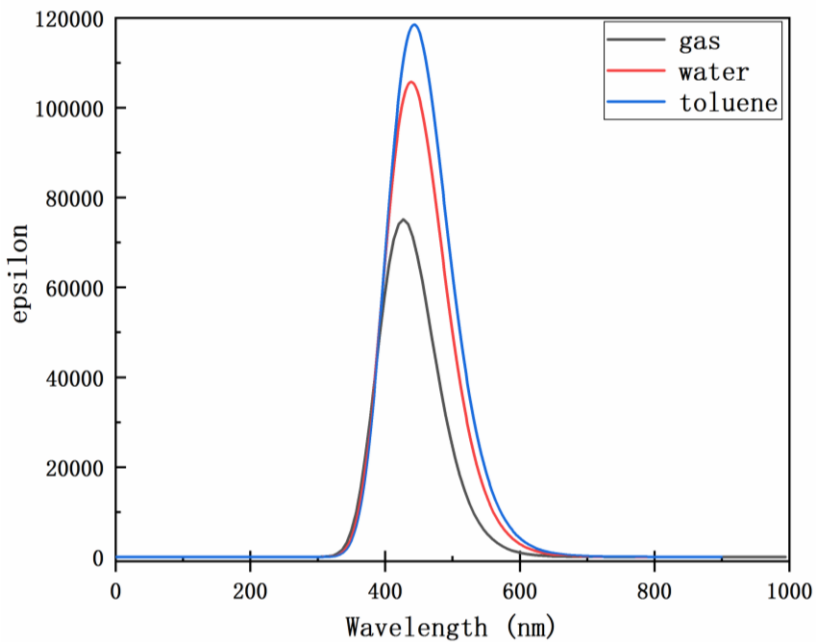


**Fig.S12** The calculated absorption spectra of the C54-GQDs dispersed in gas water and toluene.

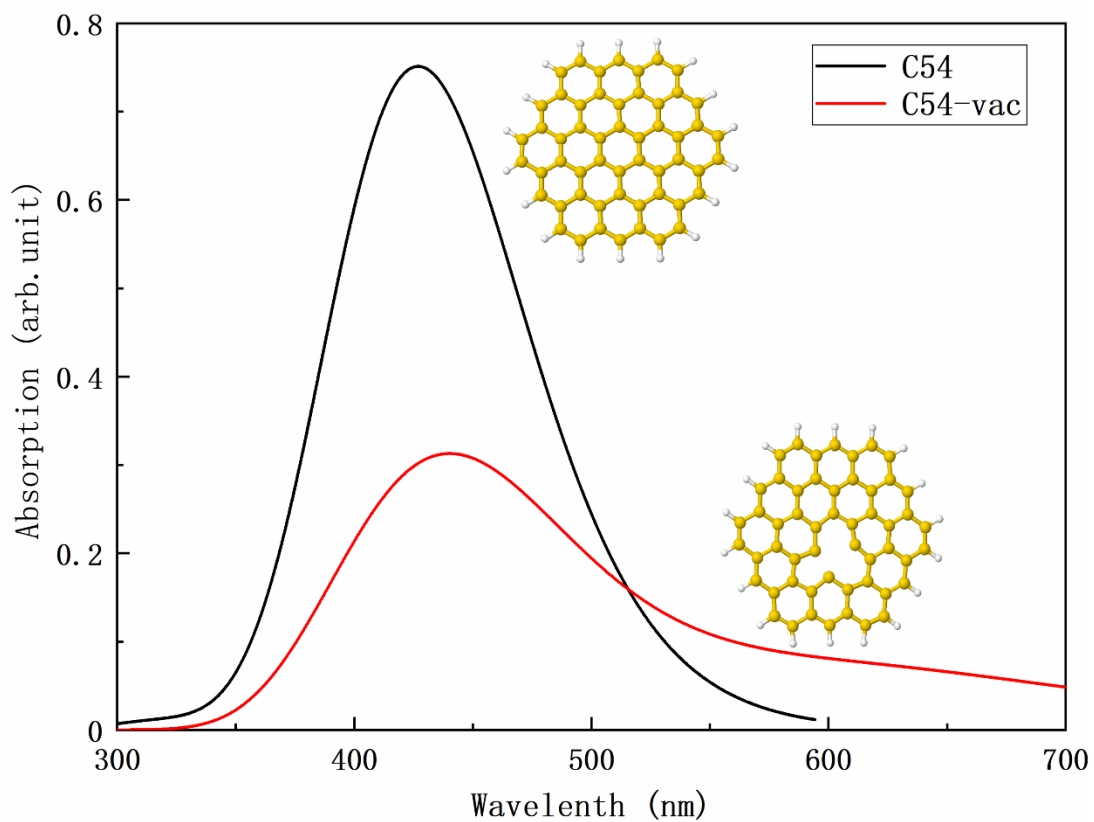


**Fig.S13** The calculated adsorption spectrum of pristine GQDs with 54 carbon atoms (54C)

and the vacancy counterpart with one missing carbon (C54-vac). The inset figure is the optimized structures of ground states. Yellow is carbon and white is hydrogen.